Estimating intracranial pressure using OCT scans of the eyeball

Eric He, Farris Atif, Nasser Al-Rayes, Zixiao Chen

NYU Center for Data Science

NYU Langone Health

Introduction

Intracranial pressure (ICP) is the fluid pressure between the skull and brain tissue. Anomalous ICP values are associated with health issues including headaches, brain swelling, blindness, and tumors. Though knowing an organism's ICP can be useful in clinical settings, directly measuring it is a dangerous and invasive procedure. This research prototypes a way to indirectly estimate ICP via its relationship with intraocular pressure (IOP), the fluid pressure inside the eye, and the lamina cribrosa (LC), a connective tissue network located at the back of the eye.

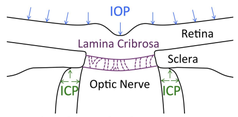

Figure 1. The relationship between ICP, IOP, and LC.

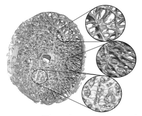

Figure 2. The lamina cribrosa is an easily deformed meshwork.

Data Preparation

Our raw data is derived from 14 rhesus monkeys. Their ICPs and IOPs were manipulated via cannulation of the eye and lateral ventricle in the brain. Scans of the optic nerve head and the LC within it were taken *in vivo* during these manipulations using optical coherence tomography (OCT), a technology commonly used in ophthalmology to produce *in vivo*, 3-D, micron-resolution scans. We thus have a 4TB dataset of LC scans where the ICP and IOP values are known. Figure 3 shows an example scan and Figure 4 depicts the cannulation process.

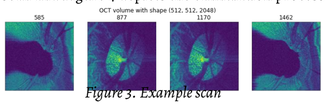

Figure 3. Example scan

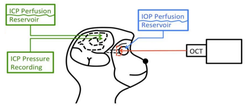

Figure 4. Cannulation of the eye and lateral ventricle

We had a number of data issues which we spent the majority of our time solving.

Missing labels The vast majority of the scans did not have IOP/ICP values. Some of these were baseline readings taken before the IOP/ICP were altered. We excluded these from the regression training set, but still used them to perform self-supervised learning. Others had their IOP/ICP values recovered from the most recent scan in which they were measured. A minority could not be inferred from the filepath or had values outside the parameter range of interest; in the end, we had 327 scans with missing IOP values and 297 scans with missing ICP values.

Scan dimensions The scan dimensions could be very different depending on the OCT machine as well as the type of scan being taken. Non-square scans (where height and width were unequal) were removed, as well as scans where the depth was too small.

Format conversion The majority of scans were in .OCT format originally and clocked in around 1GB each. We downsized all images and converted them to Torch tensors. The conversion process was rather lengthy due to the large image sizes involved.

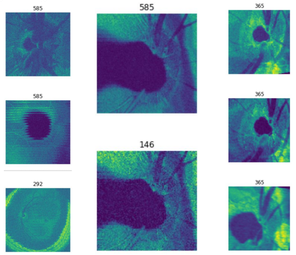

Figure 5. Image scans. By column, left to right.
(a) Scans are of varying quality.
(b) Top is original scan, bottom is downsized. No significant drop in quality observed.
(c) Random data augmentations performed dynamically during training.

Methods

Image model The fundamental building block is the 3-D ResNet which synthesizes the scan data into interpretable features for a feedforward network.
Architecture Multiple variations of 3-D ResNet, specifically ResNet10 & ResNet50, were used for this experiment.
Pretraining We initialized training from scratch as well as from pre-trained models from Tencent's MedNet trained on MRI images. The original MedNet ResNets were used for 3D segmentation, so we performed surgery on the model to get the layers we wanted.
Standardization Every image was standardized to have mean 0 and variance 1 to improve model stability. ICP and IOP values were also standardized.
Augmentation Standard techniques were applied (flips, affine transforms, blurs, Gaussian noise).
Tabular data injection The IOP data was concatenated with the image features. A single IOP value is not given much weight by the model, so we broadcast the scan's IOP value into a long tensor for concatenation. The concatenated IOP and image feature tensor feeds into a MLP which outputs the final prediction, a standardized ICP value.
Error metrics We used mean squared error for our loss function.
Hyperparameters We did not do an exhaustive hyperparameter search. We settled on an Adam optimizer with initial learning rate 3e-4.
Self-supervised learning We attempted the momentum contrastive loss ("MoCo") method to pre-train models on "pretext tasks" with the goal of forcing the model to learn a better internal representation of the images. Our pretext task is to classify whether two random crops came from the same original image.
MoCo The Resnet model is designated the "encoder", and is asked to produce an embedding for one image crop. A second "decoder" model, whose parameters are an average of the historical encoder weights, embeds a second image crop. The dot product of the two embedding tensors is fed through a sigmoid to determine the predicted probability the crops come from the same image.

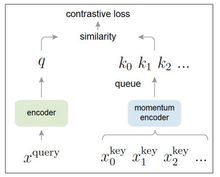

Figure 8. MoCo loss architecture

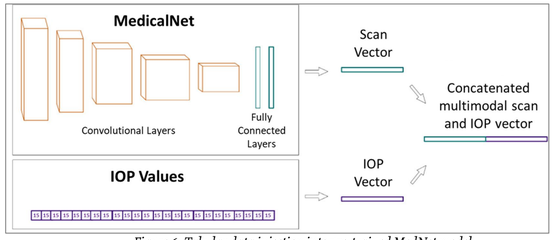

Figure 6. Tabular data injection into pre-trained MedNet model

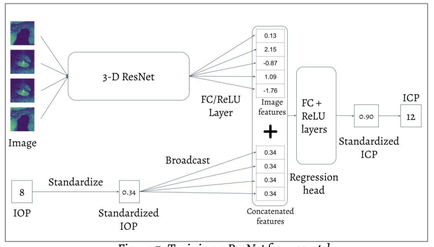

Figure 7. Training a ResNet from scratch

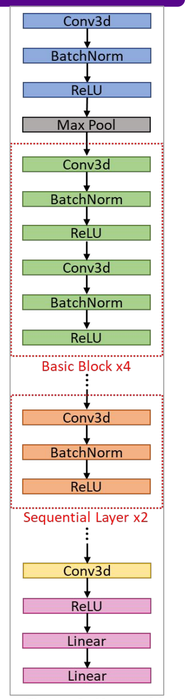

Figure 9. ResNet10 model architecture

Results

The large scale of the data as well as hardware constraints posed many challenges during modeling. As a result, batch sizes were kept relatively small (8-16) across different architectures. While initial models worked well to minimize training loss, the results weren't generalizable to holdout sets. To offset this, the input data was perturbed (bias was added), which significantly improved results when passed through ResNet50. Additionally, it was determined that the Adamax optimizer (lr 3e-4) resulted in better convergence then that of the out of box MedNet SGD. The figures below summarize the results:

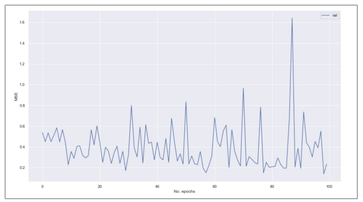

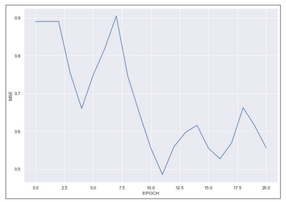

Figure 10. Validation Set Learning Curves for ResNet10 (left) and ResNet50 (right)

	Model	Augmented	Epoch #	Pretrained	Mean Validation Loss
1	ResNet50	Yes	20	No	.65
2	ResNet50	No	20	Yes	.43
3	ResNet10	Yes	100	No	.39

Figure 11. Model configuration and results

While ResNet10 minimized mean validation loss across epochs, closer analysis of the learning curves reveals model configuration 1 (ResNet50 w/ Data Augmentation) yields promising results.

Conclusion and Future Work

With a limited amount of time, we were able to restructure the large dataset and map numeric data to image scans. We also managed to build a multi-modal learning architecture by leveraging deep learning models. However, there still are lots of potential methods which we could implement and experiment with:

Change the way we predict IOP Instead of concatenating the IOP value into the network, we could have changed the prediction task to predict the ratio of the ICP to IOP; this would have obviated the need to include additional linear layers after the concatenation at the end of the network.
Try bigger models Smaller models like ResNet10 could only predict the mean, but we were able to get ResNet50 to continuously lower validation loss. Bigger models and other hyperparameters may do a better job.
Try more pretrained models MedNet was trained on MRI data, which is very different from our OCT data. We could not find recently OCT-pretrained models, but training one ourselves on larger datasets before using it for ICP prediction may have yielded a better performing model.
Solving issues with distributed training We were prevented from using MoCo only due to technical difficulties around distributed training. With such sparse data, a successfully SSL-trained model could have gotten much better results.
Model explanations The ResNet50 validation loss is still dropping; if it gave reasonably accurate predictions, explanatory methods could help understand the model better.

Acknowledgements

We would like to thank our mentor Dr. Gadi Wollstein, Dr. Narges Razavian, and our lab manager Ronald Zambrano for all their help and inspiration throughout the project. We would also like to express our gratitude for all the effort the lab put in providing us quality datasets to work with. Lastly, we would like to thank Dr. Julia Kempe for her support.

References

1. *Wang, B., Tran, H., Smith, M., Kostanyan, T., Schmitt, S., & Bilonick, R. et al. (2017). In-vivo effects of intraocular and intracranial pressures on the lamina cribrosa microstructure. PLOS ONE, 12(11), e0188302. doi: 10.1371/journal.pone.0188302*
2. *Chen, S., Ma, K., & Zheng, Y. (2019). Med3d: Transfer learning for 3d medical image analysis. arXiv preprint arXiv:1904.00625.*
3. *He, K., Zhang, X., Ren, S., & Sun, J. (2016). Deep residual learning for image recognition. In Proceedings of the IEEE conference on computer vision and pattern recognition (pp. 770-778).*
4. *Maetschke, S., Antony, B., Ishikawa, H., Wollstein, G., Schuman, J., & Garnavi, R. (2019). A feature agnostic approach for glaucoma detection in OCT volumes. PloS one, 14(7), e0219126.*
5. *He, K., Fan, H., Wu, Y., Xie, S., & Girshick, R. (2020). Momentum contrast for unsupervised visual representation learning. In Proceedings of the IEEE/CVF Conference on Computer Vision and Pattern Recognition (pp. 9729-9738).*
6. *Taleb, A., Loetzsch, W., Danz, N., Severin, J., Gaertner, T., Bergner, B., & Lippert, C. (2020). 3d self-supervised methods for medical imaging. arXiv preprint arXiv:2006.03829.*

https://github.com/Bulbasaurzc/Capstone2021